JOURNAL OF MATERIALS SCIENCE 22 (1987) 1374–1378

X-ray diffraction analysis of SiO_2 structure

B. HIMMEL, TH. GERBER, W. HEYER*, W. BLAU
Sektion Physik, Wilhelm-Pieck-Universität, Rostock, GDR
**Sektion Chemie, Martin-Luther-Universität, Halle, GDR*

The structural differences between vitreous silica and porous SiO_2 glass prepared by chemical extraction of $Na_2O \cdot B_2O_3 \cdot SiO_2$ glasses were analysed by the method of X-ray diffraction. These investigations have given evidence for regularities of continuous silica networks beyond the well known short-range order which are discussed with respect to network topology. This network topology will be considered as cristobalite-like, as demonstrated by comparison with all corresponding crystalline modifications. The significant structural differences between vitreous and porous SiO_2 were attributed to a cristobalite-like topology with high- and low-temperature character, respectively. Both structures are separated by a displacive phase transition like the α–β transition in cristobalite. This phase transition was proved by temperature-dependent *in situ* measurements of X-ray scattering.

1. Introduction

X-ray diffraction is a very useful tool for studying the structure of amorphous materials [1–6]. Such investigations provided results about fundamental structural units as well as about their connection to a three-dimensional network by yielding data on bond lengths and bond angles distributions. This information, usually obtained by Fourier transformation of the intensity curves, is not characteristic of the local network only but integrated over the whole structure. It is therefore well known [3, 7] that the short-range order of vitreous silica (v-SiO_2) is determined by regular $SiO_{4/2}$ tetrahedra such as in the corresponding crystalline modifications by the distribution of Si–O–Si bond angles varying between 120 and 180° with the most frequent value at 144° and by the rotation angles of one tetrahedron with respect to an adjacent tetrahedron, which have equal probabilities. This short-range order is supported by various continuous random networks modelled, for instance, by Bell and Dean [8]. But moreover, there is experimental evidence for a higher order in the silica network [9, 10]. None of the random bonding models can explain the form of the main peak in the silica scattering curve from which follows a maximal correlation length of 2.2 nm [9]. On the other hand, this higher order cannot be explained by small crystals connected randomly at their boundaries, as proposed earlier as a result of X-ray diffraction [11–13]. It was shown by model analysis in terms of pair distribution functions that crystallite models are not consistent with the short-range order of v-SiO_2 [14]. The existence of a phase transition in amorphous SiO_2 which is the main topic of the present study will be a further hint that there is more order in v-SiO_2 than previously assumed. We propose that the structure of v-SiO_2 is characterized mainly by a *non-random continuous* network.

2. Experimental procedure

The porous glasses used for our investigations were prepared by chemical extraction of $Na_2O \cdot B_2O_3 \cdot SiO_2$ glasses made of two different compositions:

(i) Glass A100: $Na_2O : B_2O_3 : SiO_2 = 7 : 23 : 70$ (wt %) [15].
(ii) Glass F300: $Na_2O : B_2O_3 : SiO_2 = 8 : 46 : 46$ (wt %) [16].

In order to get phase separation, Glass A100 was submitted to a thermal treatment at a temperature of 610° C for a time of 72 h before extraction of the soluble components with HCl. During a following alkaline treatment the highly dispersed SiO_2 was removed from the pores. Glass F300, containing a higher portion of Na_2O and B_2O_3, was extracted by a two-stage water–acid leaching process. Both porous glasses exhibit residual amounts of Na_2O (≈ 0.1 wt %) and of B_2O_3 (≈ 3 wt %) [17]. The measurements of porosity by mercury porosimetry yielded an average pore diameter of nearly 90 nm (A100) and 30 nm (F300), respectively [16]. These assertions were confirmed by the results of small-angle X-ray scattering [18].

All measurements of angular intensity distribution were carried out with identical collimation conditions using a symmetrical transmission technique with Ag$K\alpha$ radiation up to a maximal scattering angle of $2\theta = 120°$ (Fig. 1). The maximal value of the magnitude of the scattering vector is determined by both geometry of scattering and the wavelength λ ($s = (4\pi/\lambda) \cdot \sin\theta$, $s_{max} = 194\,nm^{-1}$). The position of this last measuring point determines the resolving limit δr of the experiment defined according to the rules of Fourier transformation [19]: $\delta r = \pi/s_{max}$. That means there can only be separated average distances between regions of different electron density greater than the resolving limit in real space. The so-called "visual field" $r_{max} = \pi/\Delta s$ of structure functions was determined by the separation of the measuring points Δs in such a way as to get structural information up to

0022–2461/87 $03.00 + .12

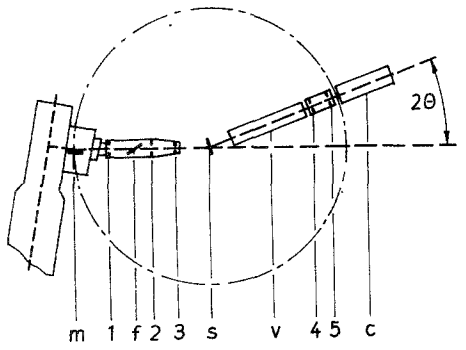

Figure 1 Collimation conditions of the wide-angle goniometer used for all investigations: (m) monochromator, (f) scattering foil for monitor signal, (s) sample, (v) vacuum chamber, (c) scintillation counter, (1) entry slit, (2) primary beam slit, (3) divergence slit, (4, 5) receiving slits.

$r_{max} = 2.6\,nm$. The interpretation of experimental results in real space takes place by discussion of the well-known radial density distribution in the representation of the difference between radial and average electron density [1]:

$$DIF(r) = \frac{2\pi}{r}\int_{s_{min}}^{s_{max}} si(s)\sin(sr)\,ds \qquad (1)$$

with

$$i(s) = \frac{I_{corr}(s) - I_{ind}(s)}{g^2(s)} \qquad (2)$$

and also by the correlation function of electron density [19]:

$$C(r) = \frac{1}{2\pi^2 r}\int_{s_{min}}^{s_{max}} I_{corr}(s)s\sin(sr)\,ds \qquad (3)$$

where $i(s)$ = reduced intensity distribution, $I_{corr}(s)$ = corrected measured intensity distribution, $I_{ind}(s)$ = independent scattering and $g(s)$ = sharpening factor [1, 2, 19].

The fundamental advantage of performing the analysis in terms of the correlation function $C(r)$ rather than $DIF(r)$ is the better ratio of useful signal to the statistical error, especially for larger r values [9].

Scattered intensities were corrected in the usual way for wide-angle diffraction [2] and normalized by comparison with the sum of coherent and incoherent independent intensities in the vicinity of large s values [20, 21]. Additionally, the distortion produced by the collimation system was removed according to Gerber [22].

All temperature measurements were made *in situ* by use of an X-ray goniometer with a furnace.

3. Results and discussion

Fig. 2 shows the s-dependent intensity distribution of v-SiO_2 cooled down under normal conditions from the melt and possessing, therefore, a fictive temperature of nearly 1400° C (Type II according to Brückner [23]) in comparison with the intensity distribution of a porous glass (F300) characterized by an average pore diameter of 30 nm. In the upper right part of this figure the first peaks are represented because, in this region, the most striking differences are seen. Firstly, the intensity of Curve 2 increases from $s = 9\,nm^{-1}$ to $s = 0\,nm^{-1}$. This remarkable small-angle scattering is caused by the high porosity of the sample. Secondly, and this should be the main point of discussion, the whole of the first peak is shifted in the direction of higher s values compared to v-SiO_2. This displacement amounts to $0.8\,nm^{-1}$. Moreover, this first peak is lower and broader in the case of porous glass, which is an indication of less order in the network structure. The absence of the two shoulders about $s = 8\,nm^{-1}$ and also about $s = 24\,nm^{-1}$ characterized by the scattering curve of v-SiO_2 (arrows in Fig. 2) is a further difference ascertainable by comparison of the first derivatives of scattering curves.

All the significant differences between the diffraction patterns can be explained by different network structures only. It should be noted that the displacement of the first scattering peak is not only a feature of anhydrous porous glass, but it was also detected in the case of amorphous colloidal SiO_2 prepared by condensation either from the vapour phase or from the solution (e.g. electron-gun evaporated SiO_2 [24], silicic acids prepared from aqueous alkali silicat solutions by precipitation and ion exchange, respectively [24], and SiO_2 gels prepared by hydrolysis and polycondensation of tetraethoxysilane [25]). Nevertheless, the angular position of the first scattering maximum of v-SiO_2 is always constant (i.e. independent of the fictive temperature of the sample). Our main intention is to find an answer to the question of how the general attribute "peak displacement" is caused by regularities of the whole SiO_2 network. The starting point should be our modern knowledge about the structure of v-SiO_2 accessible by means of wide-angle X-ray diffraction [3, 9, 10].

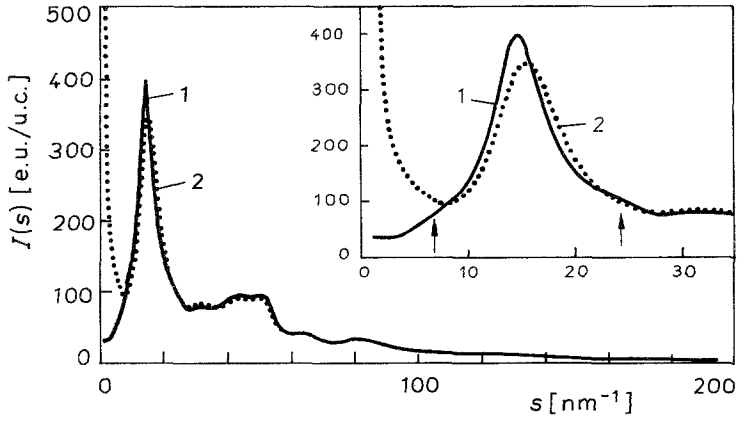

Figure 2 s-dependent intensity distribution of v-SiO_2 (Curve 1) in comparison with porous glass F300 (Curve 2); e.u./u.c. means electron units normalized to unit of composition.

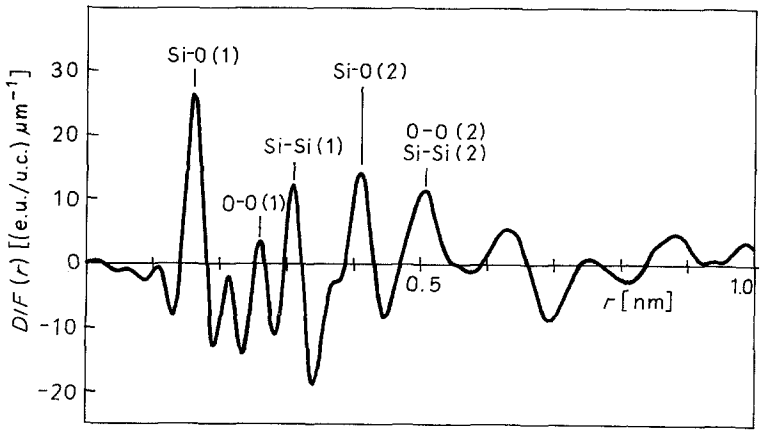

Figure 3 DIF(r) functions (Equation 1) for v-SiO_2.

Fig. 3 shows the *DIF(r)* for v-SiO_2. In accordance with the pair distribution function analysis of Mozzi and Warren [3] maxima up to $r = 0.5$ nm should be identified with average distances between the atoms in a continuous SiO_2 network inside the second coordination sphere. An identification of maxima for $r > 0.5$ nm is more complicated because of the overlapping of further contributions. It is remarkable that in contradiction to recent investigations [26, 27] maxima also for $r > 0.7$ nm were found ($r = 0.76$, 0.89 and 0.99 nm) in the structure functions (Figs 3 and 4). In Fig. 4 the correlation function of the same sample is represented for two different resolving limits. The lower resolution ($\delta r = 0.11$ nm) we obtained by transformation only of the first part of the scattering curve (insert in Fig. 2). One can see a convergent periodic oscillation vanishing at nearly 2.2 nm within the margins of error caused by the statistical error of the scattering experiment as well as by the termination effect of Fourier transformation. This oscillation becomes more structured by an improvement of the resolution. The periodicity length of the predominant oscillation with a correlation range of 2.2 nm and the presence of discrete maxima up to $r = 1$ nm are indications of a relatively regular arrangement of $SiO_{4/2}$ tetrahedra.

To get information about network topology from the period of the correlation function, we have shown by calculation of the periodicity for all crystalline modifications of SiO_2 existing under normal conditions (cristobalite, quartz, tridymite), that structural resemblance to v-SiO_2 is exhibited only for high-cristobalite (β-form). The comparison of the corresponding correlation functions (Fig. 5) of v-SiO_2 and β-cristobalite demonstrates the conformity of both periods of oscillation arising from similar structural origins in the polyhedron structure. The long-range order in the crystalline sample produces a function with increasing amplitude. It would be confirmed by an improvement of the resolving power that each peak of the correlation function of v-SiO_2 coincides with a peak of the corresponding function of β-cristobalite.

All arguments suggest that the main structural element comprising v-SiO_2 is a polyhedron (as in β-cristobalite) which consists of four six-fold rings of $SiO_{4/2}$ tetrahedra. Network defects like five-fold or seven-fold rings which must arrange in lines according to Rivier and Duffy [28] distort the polyhedra, destroy the crystalline long-range order, and result finally in a broad distribution of the Si–O–Si bond angle. It should be re-emphasized that the silica structure is characterized by a continuous network with a topology similar to that of β-cristobalite. The transformation into a lower temperature structure is hindered in the case of bulk silica by volume constraints of the three-dimensional connected network.

An important question is how the structural differences between v-SiO_2 and porous glass in real space are manifested. A comparison in terms of correlation functions is shown in Fig. 6 (Curve 1 corresponds to v-SiO_2). Because of the same peak positions up to $r = 0.41$ nm, there are no significant differences inside

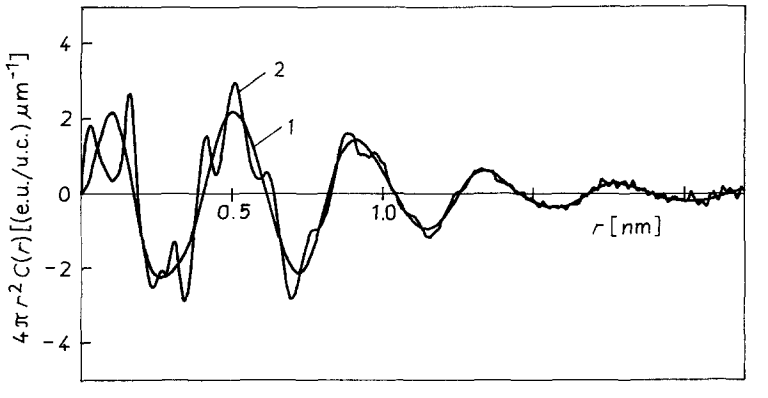

Figure 4 Correlation functions of v-SiO_2 with the resolving limits (1) $\delta r_1 = 0.11$ nm and (2) $\delta r_2 = 0.017$ nm.

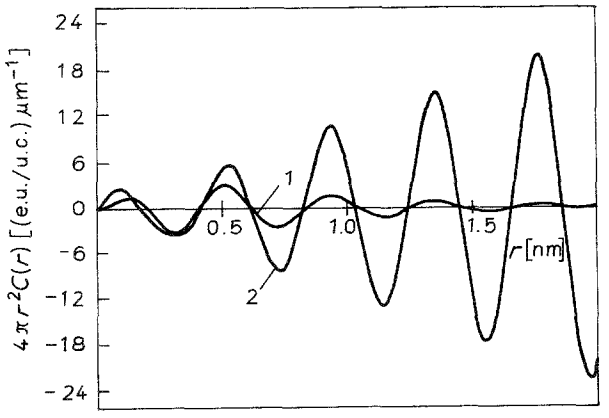

Figure 5 Comparison of correlation functions of (1) v-SiO_2 and (2) high-cristobalite with $\delta r = 0.11$ nm.

the first coordination sphere. Consequently, identical structural units ($SiO_{4/2}$ tetrahedra) build up both networks. Likewise, there is no difference between the average Si–Si bond lengths ($r = 0.31$ nm); this indicates similar average Si–O–Si bond angles. However, there must be differences in the connection of the $SiO_{4/2}$ tetrahedra to a three-dimensional network because of the different ratios of relative height of the maxima and of increasing deviations with larger distances.

The shorter period of oscillation in the case of porous glass is a consequence of a more densely packed structure and essentially it is tantamount to the peak displacement of the first scattering maximum explained previously. This displacement is comparable to the difference between the positions of the most intense crystalline reflections of α- and β-cristobalite (Fig. 7). The intensity distribution of β-cristobalite was measured at a temperature of 350° C. The transformation into the low-temperature form (α-cristobalite) takes place spontaneously by a displacive phase transition (i.e. without alteration of lattice topology and also without bond breaking), normally at a temperature of nearly 250° C [29, 30]. The actual temperature of this transformation can be modified by volume constraints or by size effects [30]. An analogous displacive phase transition was expected in the network of porous glass. To prove this hypothesis, the scattering curves of porous glass were measured at room temperature as well as at 350° C. The measurement performed at 350° C has shown that the first scattering maximum had already reached the position at $s = 15.04\,nm^{-1}$

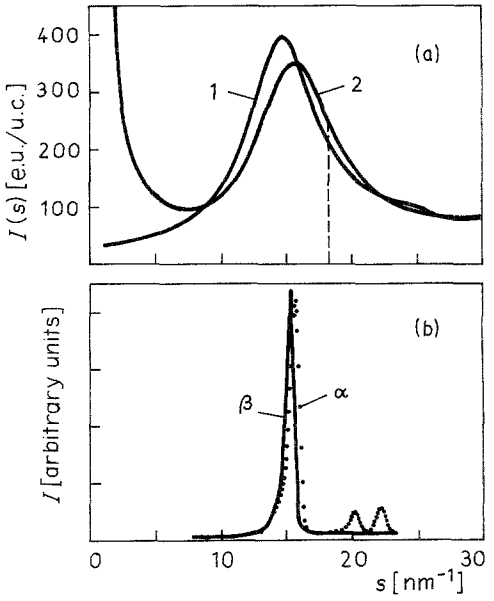

Figure 7 (a) First scattering maxima of (1) v-SiO_2 and (2) porous glass F300. (b) Representation of main peaks of the crystalline diffraction patterns for low- (α) and high-cristobalite (β).

typical for v-SiO_2. After cooling down to room temperature the original scattering curve of porous glass was obtained.

In order to get information about the transition range, temperature-dependent measurements up to $T = 350°$ C were made at a scattering angle where the largest effect was expected ($s = 18\,nm^{-1}$). The result is represented by the heating curve in Fig. 8. It took us 20 min to heat the sample up to 350° C. The decrease of intensity with increasing temperature is contingent on a displacement of the whole first maximum of the scattering curve in the direction of lower s-values caused, therefore, by a structural change in the network. This change, which was reproducible by thermal cycling, gives evidence for a reversible displacive phase transition. The average transition temperature amounts to nearly 190° C. The actual transition temperature may be modified by the porosity and by the dimensions of the regions of the SiO_2-rich matrix. The influence of the portion of highly dispersed SiO_2 within the pores on the average transition temperature should be a task of further investigations.

We consider this phase transition to be a general feature of SiO_2 networks. It is noteworthy that volume constraints, occurring in a β-cristobalite-like structure frozen in at the fictive temperature and cooled down

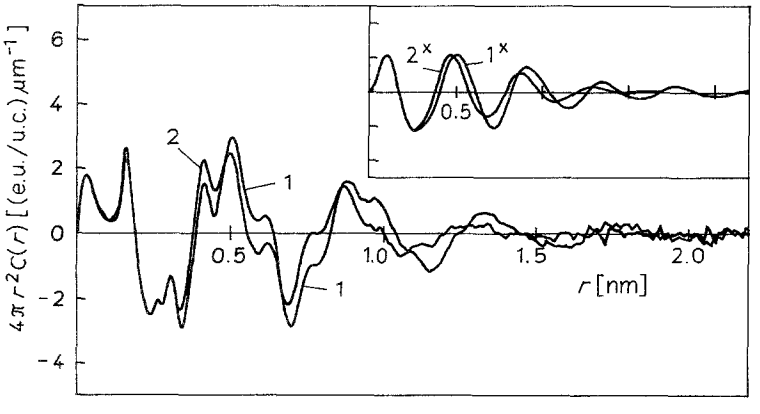

Figure 6 Correlation functions of (1) v-SiO_2 in comparison with (2) porous glass F300 for two resolving limits $\delta r = 0.017$ nm (1 and 2) and $\delta r = 0.11$ nm (1^x and 2^x).

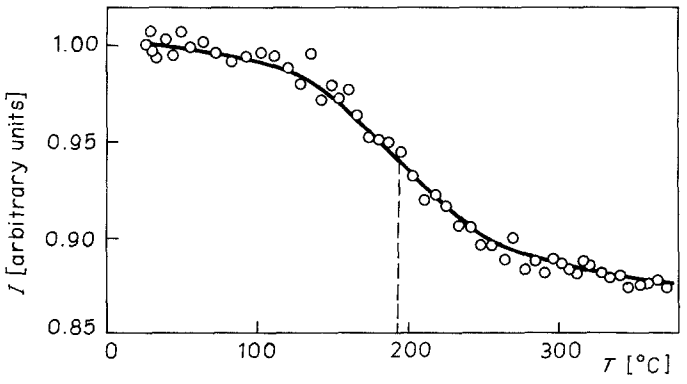

Figure 8 Change of scattering intensity with temperature at $s = 18\,nm^{-1}$ for porous glass F300.

to room temperature, hinder this phase transition. That is the reason why in all bulk silica samples, including those at room temperature, will be preserved a cristobalite topology with high-temperature character.

The other porous glass (A100), characterized by larger average pore diameters, is also an example of this behaviour. The positions of the first peaks of X-ray scattering are the same for the porous glass A100 and for v-SiO_2. Also there exist no essential differences in real space between these two SiO_2 samples detected in terms of correlation functions.

It is interesting to note that the network structures of both porous glasses are different. This indicates that the residual amounts of Na_2O and B_2O_3 cannot be the cause of the displacive phase transition in amorphous SiO_2 networks. But further investigations must follow to verify the influence of the impurity content and of the porosity on the temperature of the phase transition.

We propose that a spontaneous local displacive phase transition into the low-temperature form should be possible if network constraints were reduced by exterior influences, for instance by mechanical activation. It is more than likely that such a phase transition takes place in the regions surrounding surface defects (e.g. cracks), because there the conditions of the three-dimensional connected network are always interrupted.

4. Summary

Our investigations of the structure of vitreous silica by means of X-ray diffraction have shown that there is unambiguous indication of a higher order than the well-known short-range order in the continuous SiO_2 network. It was found by comparison with the corresponding crystalline modifications of SiO_2 in terms of correlation functions that silica structure is characterized by a continuous network with a topology similar to cristobalite. There are significant structural differences between v-SiO_2 and porous glass (F300) attributed to network structures with high- and low-temperature character, respectively. Both structures are separated by a displacive phase transition like the α–β transition in cristobalite, which was demonstrated in the case of porous glass.

References

1. B. E. WARREN, "X-ray Diffraction" (Addison-Wesley, New York, 1969) pp. 105–150.
2. H. P. KLUG and L. E. ALEXANDER, "X-ray Diffraction Procedures for Polycrystalline and Amorphous Materials" (Wiley, New York, 1974) Ch. 12.
3. R. L. MOZZI and B. E. WARREN, *J. Appl. Crystallogr.* **2** (1969) 164.
4. A. J. LEADBETTER and A. C. WRIGHT, *J. Non-Cryst. Solids* **7** (1972) 23.
5. *Idem, ibid.* **7** (1972) 141.
6. Z. BOCHYNSKI, M. STACHOWIAK and S. MOCYDLARZ, *J. Mater. Sci.* **19** (1984) 1876.
7. P. G. COOMBS, J. F. DE NATALE, P. J. HOOD, D. K. McELFRESH, R. S. WORTMAN and J. F. SHACKELFORD, *Phil. Mag. B* **51** (1985) L39.
8. R. F. BELL and P. DEAN, *Phil. Mag.* **25** (1972) 1381.
9. TH. GERBER and B. HIMMEL, *J. Non-Cryst. Solids* **83** (1986) 324.
10. R. HOSEMANN, M. HENTSCHEL, A. LANGE, B. UTHER and R. BRÜCKNER, *Z. Kristallogr.* **169** (1984) 13.
11. J. T. RANDALL, H. P. ROCKSBY and B. S. COOPER, *ibid.* **75** (1930) 196.
12. N. VALENKOV and E. A. PORAI-KOSHITS, *ibid.* **95** (1936) 195.
13. J. H. KONNERT and J. KARLE, *Acta Crystallogr.* **A29** (1973) 702.
14. H. STEIL, PhD thesis, Wilhelm-Pieck-Universität, Rostock (1979).
15. F. WOLF, F. JANOWSKI and W. HEYER, *Chem. Techn.* **28** (1976) 491.
16. W. HEYER, F. JANOWSKI and F. WOLF, *Z. Chem.* **17** (1977) 212.
17. F. JANOWSKI and W. HEYER, "Poröse Gläser" (VEB Deutscher Verlag für Grundstoffindustrie, Leipzig, 1982) Ch. 4.
18. R. KRANOLD, W. HEYER and G. WALTER, *Studia Biophys.* **98** (1983) 53.
19. R. HOSEMANN and S. N. BAGCHI, "Direct Analysis of Diffraction by Matter" (North-Holland, Amsterdam, 1962) Chs VI and VII.
20. F. HAJDU, *Acta Crystallogr.* **A28** (1972) 250.
21. G. PALINKAS and T. RADNAI, *ibid.* **A32** (1976) 666.
22. TH. GERBER, PhD thesis, Wilhelm-Pieck-Universität, Rostock (1983).
23. R. BRÜCKNER, *J. Non-Cryst. Solids* **5** (1970) 123.
24. B. HIMMEL, TH. GERBER and H.-G. NEUMANN, *Phys. Status Solidi (a)* **88** (1985) K127.
25. B. HIMMEL, TH. GERBER and H. BÜRGER, *J. Non-Cryst. Solids* (in press).
26. G. S. HENDERSON, *J. Non-Cryst. Solids* **68** (1984) 333.
27. R. N. SINCLAIR, J.-A. DESA, G. ETHERINGTON and A. C. WRIGHT, *ibid.* **42** (1980) 107.
28. M. RIVIER and D. M. DUFFY, *J. Physique* **43** (1982) 293.
29. A. J. MARJUMDAR, H. A. McKINSTRY and R. ROY, *J. Phys. Chem. Sol.* **25** (1964) 1487.
30. F. E. WAGSTAFF, *Phys. Chem. Glasses* **10** (1969) 18.

Received 5 February
and accepted 21 August 1986